Development and dosimetric evaluation of the IMRT prostate at outside-the-irradiated field in a heterogeneity male pelvis phantom

J. Jayamani[1,2] ⓘ, N. D. Osman[2], A. A. Tajuddin[3], D. O. Samson[4], K. E. Kamaruddin[1] and M. Z. Abdul Aziz[2] ⓘ

[1]School of Health Sciences, Health Campus, Universiti Sains Malaysia, 16150 Kubang Kerian, Kelantan, Malaysia; [2]Oncological and Radiological Sciences Cluster, Advanced Medical and Dental Institute, Universiti Sains Malaysia, 13200 Kepala Batas, Pulau Pinang, Malaysia; [3]Albukhary International University, 05200 Alor Setar, Kedah, Malaysia and [4]Department of Physics, University of Abuja, P.M.B 117, F.C.T., Abuja, Nigeria

CAMBRIDGE UNIVERSITY PRESS

Abstract

Background: Intensity-modulated radiation therapy (IMRT) treatment delivery requires pre-treatment patient-specific quality assurance (QA) for the dosimetry verification due to its complex multileaf-collimator movement. The prostate target close position between the bladder and rectum requires a tight margin during planning, and mistreatment would have a huge impact on the patient. A commercially available QA tool consists of a homogeneous medium and does not represent an exact photon interaction on the tumour and also on the nearby healthy organ.

Objective: A heterogeneous male pelvis phantom was developed and investigated the efficiency of the treatment planning system (TPS) calculation on the off-axis region.

Methods: Polymethyl methacrylate was used for the phantom housing, and the material closed to the bladder, rectum and prostate density was chosen to construct the organ models. The phantom was scanned and validated by the computed tomography number and density. An IMRT treatment was planned in the Monaco TPS, and a thermoluminescent dosimeter (TLD-100) was used to validate the point dosimetry. In addition, an EGSnrc Monte Carlo simulation was carried out to validate the phantom dosimetry.

Results & Discussion: The dose measurement between TLD-100, TPS, and EGSnrc was compared and validated in the pelvis phantom. In the prostate region, the dose difference was within ± 5%, and the maximum dose difference outside-the-irradiated field was up to 20·07 % and 47·31 % in TPS and TLD-100, respectively. Meanwhile, the measured dose was lower than the calculated dose, and it was apparent for the dose outside-the-irradiated field.

Conclusion: The developed heterogeneity male pelvis phantom was validated and verified to be an important QA device for validating radiation dosimetry in the pelvis region. The dose outside-the-irradiated field was underestimated by both TPS and TLD, respectively.

Introduction

The advancement of the computer technology, together with the machinery developments, external beam radiotherapy, has transformed intensely over several decades. These advancements allow the practice of more high-level treatment techniques such as intensity-modulated radiation therapy (IMRT) for cases like prostate cancer. In order to limit the radiation dose to the nearby healthy organs and tissues, a multileaf-collimator that shapes the beams and aims the radiation to the prostate from many angles and the intensity of the beams were adjusted. The IMRT implementation, however, is highly complicated and requires a severe quality assurance (QA) programme before the treatment delivery.

A pre-treatment patient-specific QA was conducted to validate the treatment plan prepared on the treatment planning system (TPS), a computer software that was used for the dosimetry calculation, and the plan was compared with the dose delivery on a linear accelerator (LINAC). Since the IMRT technique emerged in radiotherapy treatment, QA tools have been commercially available for the dosimetry verification such as Matrixx (IBA Dosimetry, GmBH, Germany), ArcCheck (Sun Nuclear, Melbourne, FL), Delta Array (ScandiDos AB, Uppsala, Sweden) and Octavious (PTW Freiburg GmbH, Germany) phantoms. This QA tool consists of a homogeneous phantom (usually $1 \, \mathrm{g \, cm^{-3}}$) with diode arrays to measure the radiation dose delivered from the LINAC. However, the composition of this homogeneous medium does not take into account on the real human body which consists of soft tissues, muscles and bony structures.

In radiation therapy, the key objective is to deliver the maximum prescribed dose to the tumour volume while to deliver the minimal radiation dose to the healthy tissues close to

Table 1. The density of human tissue and the material selected for male pelvis phantom construction. Measured value using Archimedes principle compared with the NIST X-COM value

Human tissue	Tissue density (g cm^{-3})	Phantom material	Measured density (g cm^{-3})	[a]Difference (gcm^{-3})	[a]Percentage difference (%)	NIST X-COM density (g cm^{-3})	[b]Difference (gcm^{-3})	[b]Percentage difference (%)
Skin	1·00	Polymethyl methacrylate	1·04	0·04	3·92	1·19	0·15	13·45
Bladder	0·87	Polyethylene	0·95	0·08	8·79	0·95	0	0
Prostate	1·14	Nylon	1·13	0·01	0·88	1·14	0·01	0·88
Rectum	0·63	Polyethylene	0·95	0·32	40·5	0·95	0	0

[a]difference between measured density and tissue density.
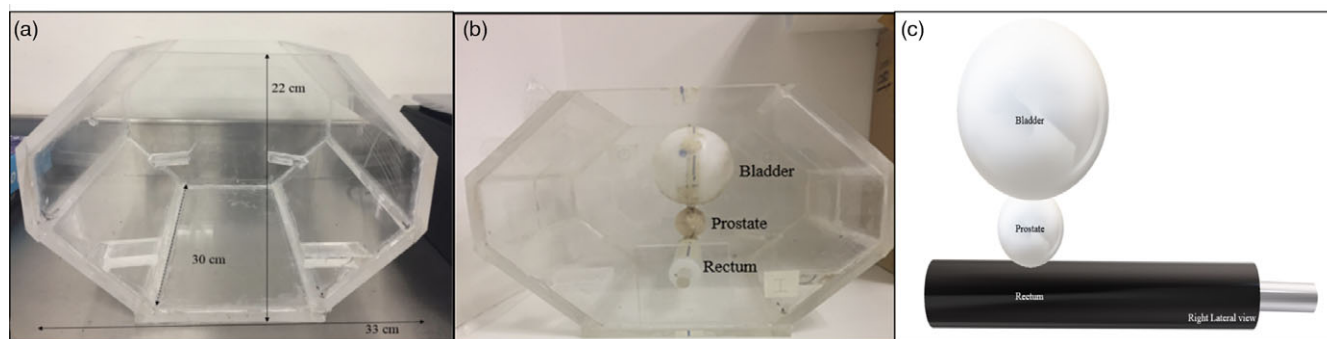[b]difference between measured density and NIST X-COM density.

Figure 1. (a) Octagon phantom housing with measurement 33 cm × 22 cm × 30 cm, and (b) organ models were inserted in the phantom housing, (c) the arrangement of the bladder, prostate and rectum in the pelvis phantom.

the tumour. Still, the healthy organs and tissues might be exposed to the unnecessary radiation dose when the radiation beam passes by or because of the scattered radiation.[1] The results of the pre-treatment QA are used to predict the treatment outcome on the patient from the alterations in the dose-volume histograms for the contoured planning target volume (PTV) and organs at risk.[2] One of the reasons for this low sensitivity is that the phantom dimension used for the pre-treatment QA is totally different from the real patients. Moreover, the depth of the dose error and the position in a patient from the QA phantom result has been difficult to evaluate. Preferably, the magnitude of the inaccuracies in the patient may stipulate more significant data than the evaluation measurement such as pass rate which depend on a standard homogeneous pre-treatment QA phantom. From these aspects, it is a challenge in pre-treatment QA to approximate the in vivo dose for the patient.

In this study, a heterogeneous male pelvis phantom was modelled and validated with the thermoluminescent dosimeter (TLD)-100 chips together with a Monte Carlo (MC) simulation. An IMRT prostate plan was delivered, and the absorbed dose was analysed at the off axis of the treatment field.

Materials and Methodology

Phantom material

The selection of the material is important to design for the function of a phantom. The purpose of the phantom material is to characterise the physical and radiological properties of tissue in the human body accurately. In this study, a phantom was modelled

to be multifunctional, where the phantom can be modified as required for specific research. Thus, a male pelvis phantom was developed to mimic a real human pelvic region, with the materials near density to the human tissue as shown in Table 1. The density was measured using an Archimedes principle, and the values were compared with the NIST X-COM database (https://physics.nist.gov/PhysRefData/XrayMassCoef/tab2.html).

Phantom geometry

The measurement of the organ was based on an Asian patient database. The detailed measurement of each organ is depicted in Fig. A1(supplementary file) with references. A sphere shape was used for the bladder and prostate with a diameter of 7 cm and 4 cm, respectively.[3,4] The length of the rectum used was 20 cm and 3 cm in diameter.[5]

The pelvis phantom housing in this study was constructed in an octagon shape with a dimension of 33 cm × 22 cm × 30 cm. This measurement was followed by a regular size of the pelvis region referring from a literature.[6] The anatomy position of the bladder, pelvis and rectum is close together; thus, these organs were constructed as attached between one and another in this developed phantom. A polymethyl methacrylate rod (ρ: 1·04 g cm^{-3}; thickness: 1 cm) was used to attach these organs. Figure 1 shows the position of these organ models' arrangement in the phantom.

Thermoluminescent dosimeter (TLD) calibration

The TLD-100 chips (Harshaw, USA) were used to determine the point dose resulting from the 6 MV exposure on the target and organ at risk in the phantom. The TLD-100 chips exhibit relative

dosimetry that follows a nonlinear dose-response along with an energy response. The TLD-100 chips require extensive labour work and are typically used where the ionisation chamber measurements were impractical especially in an anthropomorphic phantom for various dose measurements.[7] Thirty TLD-100 chips (0·3 cm × 0·3 cm × 0·1 cm) were used in this study and were calibrated under the 6 MV Elekta Synergy Agility LINAC.

Initially, the TLD-100 chips were heated under 400°C for 1 h in the annealing oven followed by rapid cooling. The annealed TLD-100 chips were irradiated under the 200 cGy at a source-to-surface distance of 100 cm, and the TLD-100 chips were positioned at a depth of 1·5 cm with a field size of 10×10 cm^2 in the solid water phantom. After 24 h, the dose response of the TLD-100 chips was measured using an automated reader, Harshaw 3500. The TLD-100 chips with ≤ 1% standard deviation were chosen for this study.[8] The sensitivity of the TLD-100 chips was calibrated in accordance with the absorbed dose to the water. The TLD-100 chips were individually numbered and irradiated in the same experimental setup to attain the individual sensitivity correction factor as defined in equation 1:

$$S_i = \frac{R_i}{\overline{R}} \tag{1}$$

where R_i is the thermoluminescent response of each TLD-100 chip and $\overline{R}$ is the mean of the responses of all TLD-100 chips. The S_i expresses the response variation of each individual dosimeter around the mean.[9]

TLD-100 position on the phantom

The developed pelvic phantom was validated for the dosimetry measurement. Thus, the phantom was allocated with a few specific points to measure the dose with the TLD-100 chips. The TLD-100 chips were grouped and labelled according to the sensitivity and placed on the prostate, bladder and rectum models. (Supplementary file: Fig. A3-A5)

Computed tomography simulation and TPS planning

Toshiba AquilionLB (Toshiba Medical System Corporation, Tochigi, Japan) computed tomography (CT) was used to scan the phantom in the pelvis routine. The parameters were set as 120 kVp, 262 mAs, and slice thickness of 2 mm was applied (to identify the TLD-100 chips position in the DICOM images), and the default kernel and the pitch factors were FC 18 and 0·69, respectively. The phantom was positioned in the centre of the CT's couch. The TLD-100 chips were placed and marked on the model of the organs in the phantom for point dose measurement in the TPS. The scanned phantom image can be seen in Figure 2 (a).

In this study, an IMRT prostate plan was constructed in the Monaco TPS (Version 5·1) using the XVMC algorithm. Following the RTOG 0126 protocol, a nine beam IMRT prostate was planned using the step-and-shoot technique with 53 segments.[10–12] The plan was optimised by 95% of the planning target volume (PTV) coverage with 95% of the prescribed dose of the 78 Gy with the lowest dose to the bladder and rectum, respectively. The conformity index value is close to 1, so it is desirable to calculate the optimum treatment plan based on the following equation:
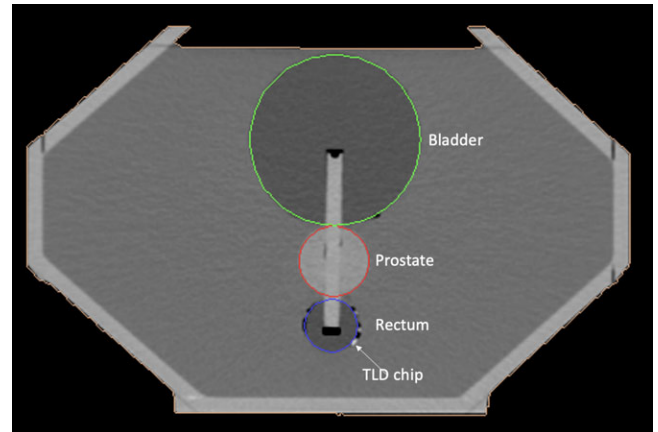

Figure 2. CT DICOM image (trans-axial view) at the isocenter point of the heterogeneity phantom in MONACO TPS in CT DICOM format. The white dot on the rectum shows the TLD-100 chip and the rod within the models is the PMMA rod that hold the organ models together.

$$CI = \frac{V_{95\%}}{\text{Volume of PTV}} \tag{2}$$

$V_{95\%}$ is the volume of PTV covered by at least 95% of the prescribed dose.

Homogeneity index (HI) has been described in the literature as a tool for evaluating dose gradients within a PTV. The HI is defined as shown in equation 3:

$$HI = \frac{D_{2\%} - D_{98\%}}{D_{50\%}} \tag{3}$$

$D_{2\%}$, $D_{98\%}$ and $D_{50\%}$ are the received dose by 2%, 98% and 50% of the target volume, and HI = 0 is a optimum value.

Monte Carlo simulation and validation

The male pelvis phantom was simulated and validated using a MC simulation, by the code of Electron Gamma Shower developed at the National Research Council of Canada (EGSnrc). This code was used to simulate a 3D model of a LINAC gantry head.[13] The Elekta Synergy Agility LINAC was modelled and validated in the recent publication.[14] Default PRESTA parameter for 6 MV photon beam was utilised with the energy cut-off for the electron, and photon was fixed to 0·7 MeV and 0·01 MeV, respectively. The phantom model was simulated in the EGSnrc code with 0·4 cm voxel size and was validated using the point dose measurement.

The LINAC model was verified with an ionisation chamber measurement (PTW farmer ionisation chamber 30,013; 0·6 cm^3 sensitive volume) to validate the EGSnrc beam model. One hundred and sixty-nine slices of the DICOM images were used to create a 3-D voxelised phantom in an '. Egsphant' file format to be used in DOSXYZnrc. The CT-CREATE (in-build software) in the EGSnrc simulation work used the CT-look-up table as given in the supplementary file (Table A1). The DICOM images in the TPS and EGSnrc are displayed in Figure 2 (a) and (b), respectively.

Dosimetry analysis

The Monaco TPS was utilised in the IMRT prostate plan, and the calculated dose on each TLD-100 chip was recorded. The Elekta

Table 2. Physical density and electron density (ED) of the materials used to model the male pelvis phantom. The percentage difference of the ED between the patient and the phantom material. Mean CT number of the phantom materials and the patient CT number. The patient data and CT number were retrieved from a (Shrotriya et al., 2018)

| Organ	Material used	Physical density (g cm^{-3})	ED (e cm^{-3})	Patient's ED (e cm^{-3})	ED difference (e cm^{-3})	Percentage difference (%)	Mean CT number (HU)	Patient CT number (HU)	Difference (HU)
Rectum	Polyethylene	0·95	0·971	1·0288	0·06	5·78	−48 ± 7	28·8 ± 14	76·8
Bladder	Polyethylene	0·95	0·971	1·0245	0·05	5·36	−46 ± 7	24·5 ± 8	70·5
Tissue	Perspex	1·04	1·018	1·0364	0·02	1·79	19 ± 8	36·4 ± 12	17·4
Prostate	Nylon	1·13	1·062	1·037	0·03	2·38	87 ± 12	31·7 ± 8	−55·3
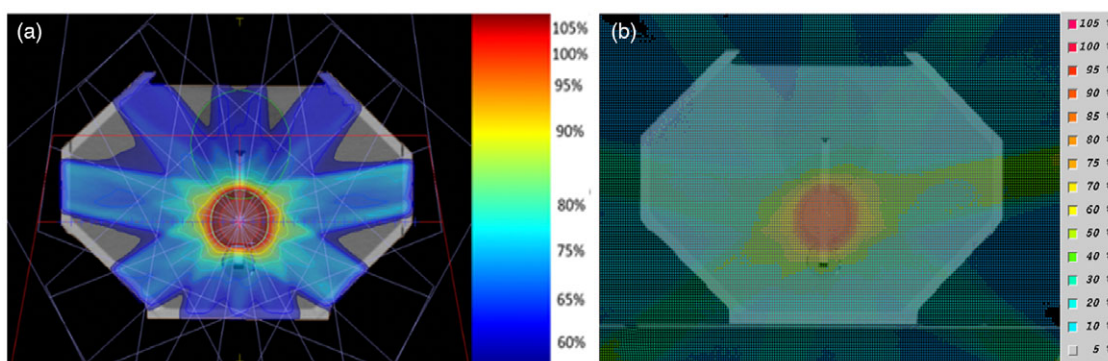
Figure 3. The transaxial view of TPS dose distribution displayed on the (a) Monaco TPS and (b) EGSnrc.

Synergy LINAC delivered the planned dose on the developed phantom with the TLD-100 chips. The exposed TLD-100 chips were analysed after 24 h of the post-irradiation using Harshaw 3500 reader. This irradiation of the TLD-100 chips was repeated three times, and the mean values were used as the relative measured dose of the TLD-100 calibration.

The phantom validation using the dosimetry comparison is part of the QA of the treatment delivery. IMRT QA reveals the variation between the measured dose and the TPS calculation delivered to the patient target volumes and organs at risk.[15] The EGSnrc Monte Carlo calculation was compared between the XVMC calculation (TPS) and TLD-100 dose measurement. Additionally, the off-axis dose on the bladder and rectum was analysed. The dose difference between the measured and the calculated dose was calculated as described in equation 4, where D_{calc} referred to the calculated dose in the TPS and TLD-100 chip measurement, while D_{MC} referred to the EGSnrc MC calculation.

$$\text{Percentage Difference}(\%) = \frac{D_{\text{calc}} - D_{\text{MC}}}{D_{\text{MC}}} \times 100\% \qquad (4)$$

Results

Phantom validation

The developed phantom was analysed based on the electron density (ED) and the CT number in Hounsfield unit (HU) of the materials that used to model the male pelvis phantom as shown in Table 2. The ED difference between the patient and the phantom was within the range of 0·02–0·06 e cm^{-3}, and the percentage difference was within 5·78% (Table 2). Table 2 stated the CT

number of materials used to simulate the various organs in the male pelvis phantom. Based on a literature report, the CT number was similar to the actual patient.[16] However, no huge difference was found for the phantom. The CT number comparison among the phantom and the patient agreed to the range between 17·4 and 76·8 HU differences.

The comparison between the density detected in the TPS and EGSnrc calculation indicates the error bar difference was within ± 5%. The density was measured along a straight line plotted as shown in supplementary file (Fig. A6). The red line indicates the CT number, and the hike in the middle reveals that the CT number of the prostate was higher than the water medium due to its density.

IMRT plan evaluation

A nine beam IMRT prostate was constructed with the isocenter at the centre of the PTV in TPS. The PTV coverage was achieved by 96·2% for the 95% of the 78 Gy prescribed dose. The conformity index was 0·95, and the homogeneity index (HI) was 0·11. The same plan was replicated in the EGSnrc simulation as shown in Figure 3 (a) and (b).

TLD-100 chip calibration

The TLD-100 chip dose-response curve was obtained for the dose range between 2 Gy and 10 Gy. The dose response of the TLD-100 chips for 6 MV photon was linear ($R^2 = 0·9906$) as depicted in supplementary file Fig. A,7 and the sensitivity of the TLD-100 was calibrated following the absorbed dose to the water. TLD-100 chips were labelled and irradiated in the same experimental setup to obtain the individual sensitivity correction factor

defined as in equation 1. The S_i expresses the response variation of each individual dosimeter around the mean. The S_i factors ranged between 0·95 and 1·05 (Supplementary file: Fig. A8). The measurements from the single TLD-100 chip were corrected for the corresponding Si factor.[9]

Dosimetry comparison

The radiation dose on the target (prostate) and the dose outside-the-irradiated volume (bladder and rectum) using the MC, TPS and TLD-100 chips on the phantom were analysed. The measured dose and TPS calculated dose were compared with the EGSnrc simulation. The result shows that the measured dose was lower than for the TPS and EGSnrc calculation on the prostate. The EGSnrc MC dose difference was within 5% difference, by 4·27% for the TPS result (Figure 4 (a)) and less than 3·2 % for the TLD dose measurement (Figure 4 (b)).

In this IMRT treatment plan, the rectum and bladder were positioned outside-the-irradiated field; thus, the radiation exposure was not directed towards it. However, both these organs are still exposed to the photon beam in a low range of radiation (following the RTOG: ASTRO FEB 2008: Low Risk). The rectum, a region below the prostate, was analysed following the TLD-100 chip position. The TLD-100 chip, TPS and EGSnrc readings were displayed in Figure 4 (c). The TLD-100 reading was below the 40% difference than the TPS calculation, and 90% of the reading was below the 40% dose difference between the TPS and EGSnrc. Figure 4 (d) indicates that the dose difference in the rectum was within 20%, except for the 7H, 7B and 7G (25·47%, 26·65% and 25·32%) in TPS, while in EGSnrc, the readings were less than 20%, except for 7H (36·45%) and 7B (27·71%) points.

The bladder, a region above the prostate (tumour target), was analysed following the TLD-100, EGSnrc MC simulation and TPS calculation. The TPS calculation shows that below the 15·22 % difference, while the TLD dose measurement indicates that the readings were below the 47·31% difference than the EGSnrc MC simulation. Figure 4 (e) and (f), the difference in bladder is also within 9% in TPS calculation, except for the points 8J, 8A and 7C (14·76%, 15·22% and 13·23%). These three TLD-100 points are located away from the treatment field, and subsequently, the deviation of the TLD dose measurement is huge. In the meantime, 8J, 7A, 5A, 8B, 8A and 7C were above 9% difference in TLD dose measurement, which were 33·18%, 47·31%, 34·9%, 16·53%, 30·92% and 28·25%, respectively.

Discussion

This phantom was designed to imitate the bladder, rectum and prostate in the male pelvis region. The materials utilised in the construction of this phantom were based on the International Commission on Radiation Units and Measurements (ICRU) report 37 recommendation.[17] This phantom was used in this study as a QA tool to verify the radiation dose calculation by the TPS.

The phantom satisfied the key criteria built up for an inter-comparison specifically, constructing with respect to a delegate male pelvis guaranteed the phantom was reasonable in size, life structures and appropriate for the assessment of the prostate radiotherapy treatment. The materials were chosen to avoid toxic or degradable properties and to be solid enough to keep up with the manufacturer's material. The materials selected to construct this phantom were close to the tissue and bone densities (< 5·78% variation) and recognisable structures in the TPS. The

CT number variation with the maximum was ± 76·8 HU for the rectum compared to the rectum's CT number published by Shrotriya (2018) in the 120 kV energy.[16] In another study that developed a pelvis phantom, the CT number of the materials was stated as prostate (1·08 ED) 75·72 HU ± 7·16, bladder and rectum material (0·97 ED) –32·54 HU ± 6 and water (1·0 ED) 1·74 HU ± 10·38 in 140 kVp scanning protocol.[18] The result matched well with the minimum variation for the phantom developed in this study since the variation of kV energy has a lower impact on the density less than 1 g cm^{-3}.[19]

To explicitly model the structure of the linear accelerator, the MC simulation is one of the precise methods for foreseeing the absorbed dose distributions which support the estimation of the clinical outcome. The MC dose computation was a significant advantage of the MC dose engine over the conventional TPS due to its lower systematic error in the dose calculation. The verification of the dosimetry accuracy with the MC simulation provides a better understanding of the dose in the inhomogeneity regions. This aiding for more precise treatment in regions that might have been difficult before by a systematic error in the dose delivery.[20] In addition, because of the absence of electron equilibrium, the benefit of MC calculation on dose prediction in areas where the dose measurements were impracticable or less accurate. In this study, the EGSnrc MC simulation showed that the density detected on the TPS was close to the phantom created in the '.egsphant' file with a variance of < ± 5%.

The phantom was designed to position the TLD-100 chips, where the TLD-100 performs well for the dose measurement in radiotherapy field.[21] In this study, the TLD chips were used in the IMRT prostate plan for the evaluation. The typical agreement between the TLD-100 chip measurements and the TPS calculation values was within ± 5% difference with the exemption of a few points far off axis, near the high dose gradient region at the surface of the phantom.[18,22]

The percentage difference (EGSnrc MC compared with the TLD-100 and TPS) of TLD-100 in the out-of-field position, where the bladder was 15·22 % in TPS and 47·31 % in TLD-100, while the rectum was 20·07 % and 38·05% in TPS and TLD-100, respectively. The discrepancy between the TPS and EGSnrc was quite close because the calculation algorithm was voxel-based Monte Carlo (XVMC) in Monaco TPS, and the EGSnrc MC algorithms were developed by the Kawrakow.[23] The out-of-field measurements were in a low-dose region, and as a result, the statistical difference in the dose measurement was massive relative to the dose received.

The percentage of dose difference in the bladder and rectum was 58% and 42%, respectively, which passed the 20% dose difference criteria in TLD-100, while TPS dose differences in both bladder and rectum were below 20%. In an IMRT TPS dose validation, the irradiations passed the narrowed TLD-100 with the dose error of less than 5% with the EGSnrc simulation; however, the TPS result shows higher dose calculation with the difference up to 6·5% with the TLD-100, and the significant amount of the failures was originating from the essentials of the TPS commissioning itself.[24] The accepted difference in the raw response of the individual TLD-100 chip from the average of the batch was compared, and a deviation of less than ± 20% was considered within the tolerance level.[25] An acceptance of 10% variation was subsequently considered appropriate for the measurement of the absorbed dose.[26] However, it was recommended by the ICRU that the dose delivered should be within 5% of the prescribed dose in the target volume.[27] Meanwhile, the Imaging and Radiation Oncology Core Houston used the 7% criterion for the TLD-100 in the PTV.[28,29]
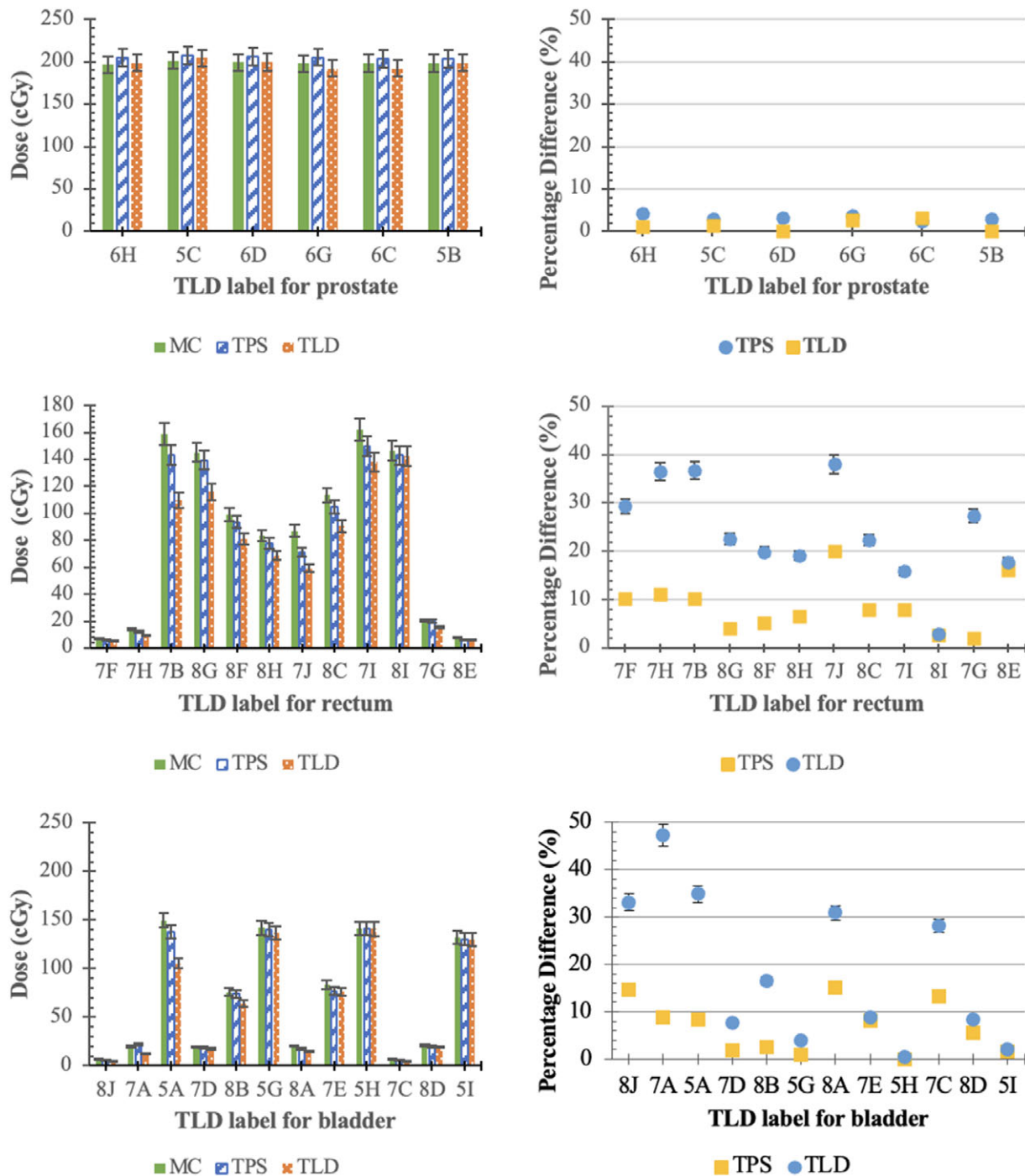
Figure 4. The measured dose (TLD) and calculated dose (TPS and EGSnrc) for the selected points in (a) prostate, (c) bladder and (e) rectum in the phantom. The relative dose difference for TPS and EGSnrc was calculated relative to measure dose (TLD) in (b) prostate, (d) bladder and (f) rectum.

In most of the cases, calculated dose for large dose gradient regions like the build-up region has high deviation. This is acknowledged by the TPS commissioning and QA protocols, which recommend an acceptance limit of up to 20% deviation in these regions. The TPS overestimated the radiation dose compared to the TLD-100 chip measurements.

The level of accuracy is most important in dose delivered to the patient, and it is the goal of the radiation therapy. But the fact is that the accuracy of 2% to 3% of the dose delivered to the patient is very challenging, especially with today's advanced technology in

the dose delivery. The principles of tolerability had been defined based on the IAEA TRS-430, and it is acceptable between 2% and 5% dose, depending on the tumour location, the beam geometry and the supplementary accessories used in the treatment. The findings were within the IAEA acceptance limit of 5% in 84% of the cases, whereas 1·3% had divergences greater than 20%, pointing out major issues in the dose delivery to the TLD-100 chip.[30] TLD-100 dose measurement was based on the TPS calculation, where EGSnrc was able to calculate the dose without any restriction. Thus, in this study, we found that, in target volume (PTV), the

dose calculated by the TPS was delivered exactly by the TLD-100 measurement and was validated by the EGSnrc MC calculation. However, the dose out-of-field is not predicted well by the TLD since it is referring to the TPS calculation with the restriction for the out-of-field. The EGSnrc MC calculation depicted the exact dose that should be calculated by the TPS, by having a large deviation.

Conclusion

A novel male pelvis phantom has been established with the ability to perform a dosimetric evaluation with a 5% dose difference within the treatment field. The TLD-100 chip measurement was lower than the calculated dose with a 5% difference in the treatment target region with the closest result to EGSnrc MC. However, in the out-of-treatment region, the measured dose was lower than the EGSnrc MC calculated dose by 47·31% and 38·05% in the bladder and rectum, respectively. This concludes that the out-of-field dose from the EGSnrc and TPS should only be used with a clear understanding of the inaccuracy of the dose calculations beyond the edge of the treatment field.

References

1. Khabaz R. Phantom dosimetry and cancer risks estimation undergoing 6 MV photon beam by an Elekta SL-25 linac. Appl Radiat Isot 2020; 163: 109232.
2. Kamomae T, Shimizu H, Nakaya T et al. Three-dimensional printer-generated patient-specific phantom for artificial in vivo dosimetry in radiotherapy quality assurance. Physica Medica 2017; 44: 205–211.
3. Zhang S-J, Qian H-N, Zhao Y et al. Relationship between age and prostate size. Asian J Androl 2013; 15: 116–120.
4. Lurie KL, Smith GT, Khan SA et al. Three-dimensional, distendable bladder phantom for optical coherence tomography and white light cystoscopy. J Biomed Opt 2014; 19: 036009.
5. Williams D, Kenyon A, Adamson D. Physiology. In: Bennett P, Williamson C (eds.). Basic Science in Obstetrics and Gynaecology: A Textbook for MRCOG Part I. 4th Edition. Churchill Livingstone, 2010: 173–230.
6. Cunningham JM, Barberi EA, Miller J et al. Development and evaluation of a novel MR-compatible pelvic end-to-end phantom. J Appl Clin Med Phys 2019; 20(1): 265–275.
7. Low DA, Moran JM, Dempsey JF et al. Dosimetry tools and techniques for IMRT. Medical Physics 2011; 38: 1313–1338.
8. Elcim Y, Dirican B, Yavas O. Dosimetric comparison of pencil beam and Monte Carlo algorithms in conformal lung radiotherapy. J Appl Clin Med Phys 2018; 19: 616–624.
9. Liuzzi R, Savino F, D'Avino V et al. Evaluation of LiF:Mg,Ti (TLD-100) for intraoperative electron radiation therapy quality assurance. Multhoff G (ed.). PLOS ONE 2015; 10: e0139287.
10. Kung JH, Reft C, Jackson W et al. Intensity-modulated radiotherapy for a prostate patient with a metal prosthesis. Med Dosim 2001;26: 305–308.
11. Su A, Reft C, Rash C et al. A case study of radiotherapy planning for a bilateral metal hip prosthesis prostate cancer patient. Med Dosim 2005; 30: 169–175.
12. Hayashi A, Shibamoto Y, Hattori Y et al. Dose volume histogram comparison between static 5-field IMRT with 18-MV X-rays and helical tomotherapy with 6-MV X-rays. J Radiat Res 2015; 56: 338–345.
13. Kawrakow I, Mainegra-Hing E, Rogers DWO et al. The EGSnrc Code System: Monte Carlo Simulation of Electron and Photon Transport. National Research Council Canada (NRCC), Ottawa, Canada, 2018.
14. J. Jayamani, N. D. Osman, A. A. Tajuddin et al. Dosimetric comparison between Monaco TPS and EGSnrc Monte Carlo simulation on Titanium Rod in 12bit and 16bit image format. J Radiat Res Appl Sci 2020; 13: 496–506. DOI: 10.1080/16878507.2020.1754042.
15. Zhang M, Qin S, Chen T et al. A clinical objective IMRT QA method based on portal dosimetry and electronic portal imager device (EPID) measurement. Technol Cancer Res Treat 2012; 12. DOI: 10.7785/tcrt.2012.500314.
16. Shrotriya D, Yadav RS, Srivastava RNL et al. Design and development of an indigenous in-house tissue- equivalent female pelvic phantom for radiological dosimetric applications. Iranian J Med Physics 2018; 15. DOI: 10.22038/ijmp.2018.26717.1274.
17. Berger MJ, Inokuti M, Anderson HH et al. ICRU report 37. J Int Comm RadiatUnits Measurem 1984;os19:NP-NP.
18. Harrison KM, Ebert MA, Kron T et al. Design, manufacture, and evaluation of an anthropomorphic pelvic phantom purpose-built for radiotherapy dosimetric intercomparison. Med Phys 2011; 38: 5330–5337.
19. Afifi MB, Abdelrazek A, Deiab NA et al. The effects of CT x-ray tube voltage and current variations on the relative electron density (RED) and CT number conversion curves. J Radiat Res Appl Sci 2020; 13: 1–11.
20. Haga A, Magome T, Takenaka S et al. Independent absorbed-dose calculation using the Monte Carlo algorithm in volumetric modulated arc therapy. Radiat Oncol 2014; 9: 75.
21. Kry SF, Bednarz B, Howell RM et al. AAPM TG 158: measurement and calculation of doses outside the treated volume from external-beam radiation therapy. Med Phys 2017; 44: e391–429.
22. Bencomo JA, Chu C, Tello VM et al. Anthropomorphic breast phantoms for quality assurance and dose verification. J Appl Clin Med Phys 2004; 5: 36–49.
23. Kawrakow I, Fippel M. Investigation of variance reduction techniques for Monte Carlo photon dose calculation using XVMC. Phys Med Biol 2000; 45: 2163–2183.
24. Smilowitz JB, Das IJ, Feygelman V et al. AAPM medical physics practice guideline 5.a.: commissioning and QA of treatment planning dose calculations - megavoltage photon and electron beams. J Appl Clin Med Phys 2015; 16: 14–34.
25. Ebrahim Ahmed AA. Study of Physical Factors Affecting the TLD Readout. 2015.
26. Akpochafor MO, Aweda MA, Ibitoye ZA et al. Thermoluminescent dosimetry in clinical kilovoltage beams. Radiography 2013; 19: 326–330.
27. Nath R, Biggs PJ, Bova FJ et al. AAPM Code of Practice for Radiotherapy Accelerators: Report of AAPM Radiation Therapy TG45. New York, United States of America, 1994.
28. Kry SF, Molineu A, Kerns J et al. Institutional patient-specific IMRT QA does not predict unacceptable plan delivery. Int J Radiat Oncol Biol Phys 2014; 90: 1195–1201.
29. Miften M, Olch A, Mihailidis D et al. Tolerance limits and methodologies for IMRT measurement-based verification QA: recommendations of AAPM task group No. 218. Med Phys 2018; 45: e53–83.
30. van Dyk J, Battista JJ, Bauman GS. Accuracy and uncertainty considerations in modern radiation oncology. In: van Dyk J (ed.). The Modern Technology of Radiation Oncology. Medical Physics Publishing, Madison, Wisconsin, 2013.